Counting Classical Nodes in Quantum Networks

He Lu,[1,2,3,§] Chien-Ying Huang,[4,§] Zheng-Da Li,[1,2] Xu-Fei Yin,[1,2] Rui Zhang,[1,2] Teh-Lu Liao,[4] Yu-Ao Chen,[1,2,*] Che-Ming Li,[4,5,6,†] and Jian-Wei Pan[1,2,‡]

[1]*Shanghai Branch, National Laboratory for Physical Sciences at Microscale and Department of Modern Physics, University of Science and Technology of China, Shanghai 201315, China*

[2]*Synergetic Innovation Center of Quantum Information and Quantum Physics, University of Science and Technology of China, Hefei, Anhui 230026, China*

[3]*School of Physics, Shandong University, Jinan 250100, China*

[4]*Department of Engineering Science, National Cheng Kung University, Tainan 701, Taiwan*

[5]*Center for Quantum Frontiers of Research & Technology, National Cheng Kung University, Tainan 701, Taiwan*

[6]*Center for Quantum Technology, Hsinchu 30013, Taiwan*

(Received 22 April 2019; accepted 8 April 2020; published 7 May 2020)

Quantum networks illustrate the use of connected nodes of quantum systems as the backbone of distributed quantum information processing. When the network nodes are entangled in graph states, such a quantum platform is indispensable to almost all the existing distributed quantum tasks. Unfortunately, real networks unavoidably suffer from noise and technical restrictions, making nodes transit from quantum to classical at worst. Here, we introduce a figure of merit in terms of the number of classical nodes for quantum networks in arbitrary graph states. Such a network property is revealed by exploiting a novel Einstein-Podolsky-Rosen steerability. Experimentally, we demonstrate photonic quantum networks of n_q quantum nodes and n_c classical nodes with n_q up to 6 and n_c up to 18 using spontaneous parametric down-conversion entanglement sources. We show that the proposed method is faithful in quantifying the classical defects in prepared multiphoton quantum networks. Our results provide novel identification of generic quantum networks and nonclassical correlations in graph states.

DOI: 10.1103/PhysRevLett.124.180503

Quantum mechanics enables nonclassical correlations to exist across the whole of a network via connecting individual quantum nodes, forming a joint quantum many-body system [1]. Quantum networks [2,3] have far greater capacity than the classical ones and serve as well-advanced transmitters of quantum information for all the distant network participants. Such utilities encourage important applications in distributed quantum information processing, from quantum secret sharing (QSS) [4–9] to distributed sensing [10,11], and from distributed quantum computation [12–15] to quantum conference key agreement and distribution [16–18]. The physical realization of these distributed quantum tasks requires suitable connectivities between nodes and network topologies to initialize the nodes in the multipartite entangled states, known as *graph states* [19] [see Fig. 1(a)].

To establish a quantum network in graph states with tailored topology, quantum information demands to be sent, received, stored, and exchanged between remote quantum nodes via photonic channels in general [1–3,32–41]. Then, it is essential to characterize a created network before it carries out a given distributed task, such as a QSS scheme. A conventional way to detect entanglement in the laboratory is an entanglement witness (EW), which employs deduction from the predictions of quantum theory [42–44]. However, inevitable imperfections of network nodes, such as the intrinsic fragility of quantum systems and errors present in actual implementations, can cause quantum nodes to become classical systems that obey the laws of classical physics, therefore leading to the failure of state preparation or decay of quantum networks [1–3,32–41]. Moreover, when network participants only have limited knowledge about the node imperfections, the network nodes then become untrusted to the participants as untrusted nodes. Considering the existence of untrusted nodes in the created network, the EW is no longer reliable in verification of multipartite entanglement. This raises a natural question: How can a verifier, such as the dealer in QSS, objectively and reliably detect the presence of classical nodes in a given network for distributed tasks?

In this Letter, we address this issue by exploiting a novel Einstein-Podolsky-Rosen (EPR) steerability [21–23], which is capable of excluding the existence of classical nodes in quantum networks. More importantly, the EPR steerability presents more fine-grained information about the created network, i.e., the capability of counting the number of classical nodes in the created network, which is not possible in other schemes [44,45].

Given an ideal N-node quantum network in arbitrary graph state $|G\rangle$, where each node contains a qubit, its general state decomposition can be explicitly expressed as [24,25]

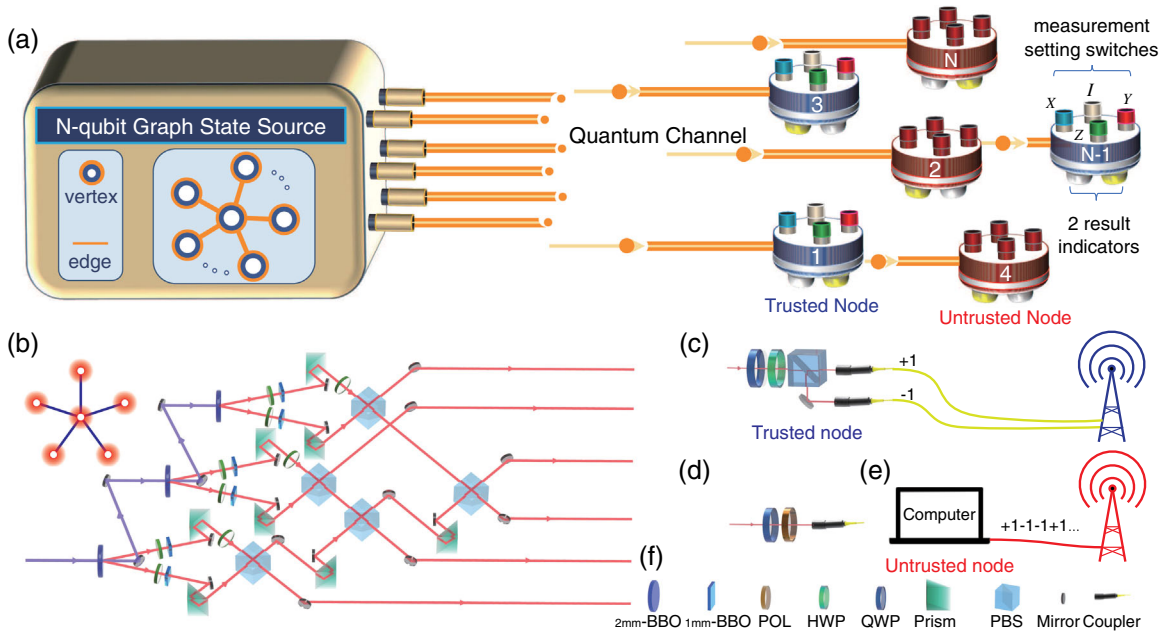

FIG. 1. Schematic drawing of the quantum network in a graph state and its experimental realization. (a) A quantum network ideally prepared in a graph state is depicted using the graph $G(V, E)$ [19,20]. The graph G consists of the vertex set V and the set E of edges each of which joins two vertices. The vertices and the edges physically represent the qubits and the interacting pairs of qubits respectively, and then constitute a state vector $|G\rangle$ of the network. A quantum network in the graph state $|G\rangle$ is then distributed to distant nodes and verified by measurement apparatus. The measurement setting is chosen from set $\{I, X, Y, Z\}$, each of which has two outcomes $+1$ and -1. The blue (red) measurement apparatus represents trusted (untrusted) nodes in the quantum network. It has been shown that arbitrary graph states among the network participants for distributed tasks can be established through a modular and plug-and-play architecture [32]. (b) The experimental setup to generate a six-photon state in a star graph, which is equivalent to $|\mathrm{GHZ}\rangle_6$ via LOCC. (c) The experimental setup to measure network fidelity F. (d) The experimental setup to generate the state in the optimal "cheating strategy," in which we project one photon on $|\xi'\rangle$ according to the target state $|G\rangle$. (e) the untrusted node broadcasts results according to the measurement setting of $F(6)$ [20,29,30]. (f) Symbols used in (b), (c), and (d): 2 mm-long BBO crystal (2 mm-BBO), 1 mm-long BBO crystal (1-mm BBO), polarizer (POL), half-wave plate (HWP), quarter-wave plate (QWP), and polarization beam splitter (PBS).

$$|G\rangle\langle G| = \sum_{\vec{m}} h_{\vec{m}} \bigotimes_{k=1}^{N} \hat{R}_{m_k}, \tag{1}$$

where $h_{\vec{m}}$ are coefficients and $\hat{R}_{m_k}$ represents the m_kth observable of the kth node. We then introduce the network fidelity function for arbitrary target graph states $|G\rangle$ of N nodes

$$F(N) = \sum_{\vec{m}} h_{\vec{m}} \langle R_{m_1} \cdots R_{m_N} \rangle \tag{2}$$

where $\vec{m} \equiv (m_1, \ldots, m_N)$ and R_{m_k} is the outcome of the m_kth measurement of $\hat{R}_{m_k}$ on the kth node. In our study, the measurements on each qubit are performed with the observables in Pauli matrices, $\{\hat{R}_{m_k} | m_k = 0, 1, 2, 3\}$, where $\hat{R}_0 = I, \hat{R}_1 = X, \hat{R}_2 = Y$, and $\hat{R}_3 = Z$. Note that the fidelity function [Eq. (2)] is state dependent and we obtain $F = 1$ for an ideal quantum network regardless of what fidelity function is chosen. We utilize the network fidelity function, which measures the closeness of created networks and target graph states, as the basis for counting classical nodes. This makes our framework capable of being used in a wide variety of circumstances and applications based on the fidelity measure.

When classical nodes exist in the created network, the network becomes a hybrid system consisting of n_q quantum nodes and n_c classical nodes, where $N = n_q + n_c$. The index set of the network nodes, V, can then be divided into the quantum-node subset, V_Q, and the classical-node subset, V_c, accordingly. An essential difference between quantum and classical nodes is that physical properties of quantum nodes might not have definite values. In contrast, variables in classical nodes are in existing states independent of observation, known as the assumption of *realism* [26,46,47]. In our framework, a node is defined as being *classical* if, for any physical properties of interest, it is classical realistic, i.e., the state of each classical node can be specified by a preexisting and fixed set of measurement outcomes [23]. Note that with the increase of noises, the quantum nodes can eventually be described by the classical realistic theory. See Supplemental Material (SM) for detailed discussion of classical nodes [20].

Before the state decays, the state vector of the target graph state can always be represented in the Schmidt form of rank r [27]

$$|G\rangle = \frac{1}{\sqrt{r}} \sum_{v=0}^{r-1} |v\rangle_{sQ} |v\rangle_{sc}, \tag{3}$$

for $r \geq 2$, where $\{|v\rangle_{sQ}\}$ and $\{|v\rangle_{sc}\}$ are the Schmidt bases for the nodes in the vertex sets V_Q and V_c, respectively. This representation shows us the following form under the state decomposition [Eq. (1)] for the nodes in V_c:

$$|G\rangle\langle G| = \frac{1}{r} \sum_{v,v',\vec{m}_c} h_{\vec{m}_c}^{vv'} |v\rangle_{sQsQ}\langle v'| \bigotimes_{k\in V_c} \hat{R}_{m_k}, \tag{4}$$

where $|v\rangle_{scsc}\langle v'| = \sum_{\vec{m}_c} h_{\vec{m}_c}^{vv'} \bigotimes_{k\in V_c} \hat{R}_{m_k}$, $\vec{m}_c \equiv \{m_k | k \in V_c\}$, and $h_{\vec{m}_c}^{vv'}$ denote the decomposition coefficients. With the classical realistic theory for a complete description of the total state of the n_c classical nodes in terms of the preexisting outcome sets: $\{\mathbf{v}_k | k \in V_c\}$, the network fidelity function [Eq. (2)] can be rephrased as the following explicit form:

$$F = \frac{1}{r} \sum_{v,v',\vec{m}_c} h_{\vec{m}_c}^{vv'} \langle |v\rangle_{sQsQ}\langle v'| \rangle \left\langle \prod_{k\in V_c} R_{m_k} \right\rangle. \tag{5}$$

The maximum fidelities between target graph states $|G\rangle$ and N-node networks having n_c classical nodes can then be described by the equation

$$\mathcal{F}_{n_c} = \frac{1}{4}(1 + 2^{-n_c/2}\sqrt{4 + 2^{n_c}}), \tag{6}$$

where $1 \leq n_c \leq N-1$, holding for arbitrary target graph states (see SM for the detailed derivation [20]). The threshold fidelities $\mathcal{F}_{n_c}$ strictly decrease with the number of classical nodes n_c. It turns out that there exists a one-to-one correspondence between the number of classical nodes and the relevant maximum fidelity values. For instance, $\mathcal{F}_1 \simeq 0.6830$, $\mathcal{F}_2 \simeq 0.6036$, and $\lim_{n_c\to\infty} \mathcal{F}_{n_c} \simeq 0.5000$. The hybrids of quantum and classical nodes are then comparable in fidelity to the networks composed entirely of quantum nodes with $F \leq \mathcal{F}_1$. This implies that the collection $\{\mathcal{F}_{n_c}\} \equiv \{\mathcal{F}_{n_c} | n_c = 1, 2, \ldots, N-1\}$ of the threshold fidelities can serve as a set of graduations to indicate the degree of network imperfection. That is, if the measured fidelity F is found to be $\mathcal{F}_{n_c'+1} < F \leq \mathcal{F}_{n_c'}$, then one can infer that there are n_c' classical nodes in the created network. Note that the preexisting state model used here is distinct from hidden variable models, such as the Mermin-Peres square, where noncontextual outcomes apply to each of nine observables for the tests of state-independent quantum contextuality in two-qubit systems [46,48–52]. By contrast, our quantum-classical hybrid model for the derivation of $\mathcal{F}_{n_c}$ combines both preexisting outcomes from n_c classical nodes and quantum measurements performed in n_q quantum nodes.

Indeed, the collection $\{\mathcal{F}_{n_c}\}$ quantitatively describes how the nonclassical correlations among nodes of the graph states vary between the quantum-classical hybrids. If $F > \mathcal{F}_{n_c}$ for a created network, then it is impossible to simulate the correlations between nodes using any networks mixed with classical defects of the minimum classical nodes, n_c. Such a quantum characteristic can be interpreted as the genuine multi-subsystem EPR steering [20], a new type of genuine multipartite EPR steerability [28] of graph states [23]. Notably, the new-found criterion $F > \mathcal{F}_{n_c}$ is stricter than EW $F > 1/2$ for genuine multipartite entanglement [42–44] of networks, in which a network containing classical nodes can mimic the networks with genuine multipartite entanglement to show $1/2 < F < \mathcal{F}_1$. This serious flaw makes the EW unreliable in the verification of genuine multipartite entanglement for distributed quantum tasks.

We experimentally demonstrate our protocol on multipartite graph states in a star graph $|G_N^{\text{star}}\rangle$, which is equivalent to a Greenberg-Horne-Zeilinger (GHZ) state $|\text{GHZ}\rangle_N = (1/\sqrt{2})(|0\rangle^{\otimes N} + |1\rangle^{\otimes N})$ via local operation and classical communication (LOCC). The experimental setup to generate a six-photon GHZ state $|\text{GHZ}\rangle_6 = (1/\sqrt{2})(|H\rangle^{\otimes 6} + |V\rangle^{\otimes 6})$ with H the horizontal polarization and V the vertical polarization is shown in Fig. 1(b). An experimental state, denoted as ρ_6^{GHZ}, is generated by employing the typical spontaneous parametric down-conversion entangled photon source and photonic interferometry technologies (see SM for more details [20]). The network fidelity $F(6)$ of the generated state ρ_6^{GHZ} is measured by the device shown in Fig. 1(c), which is consisted of a quarter-wave plate (QWP), half-wave plate (HWP), a polarization beam splitter (PBS), and two detectors. By properly choosing the angle of the QWP and HWP, the expected value of I, X, Y, and Z can be readout. The experimental results of measured $F(6)$ are shown in Fig. 2(a), from which we calculate that $F(6) = 0.792 \pm 0.006$ [shown with blue bar in Fig. 2(c)]. Then $F(6)$ exceeds the threshold fidelity $\mathcal{F}_1 = 0.683$ by more than 18 standard deviation, which indicates there is no classical node in the tested network.

We then consider the case where n_c classical nodes exist in the N-node network, and show that $F(N)$ is bounded by the threshold fidelity $\mathcal{F}_{n_c}$ even with the optimal "cheating strategy" (OCS). The OCS of one untrusted node in bipartite quantum correlation has been well discussed [53]. We generalize the OCS of n_c untrusted (classical) nodes existing in N-node network as: the n_c untrusted nodes first prepare the entangled state $|\xi\rangle_{n_q}$ for n_q trusted (quantum) nodes based on their knowledge of the N-node network, where $n_q = N - n_c$. Then, according to the measurement setting for the network fidelity function

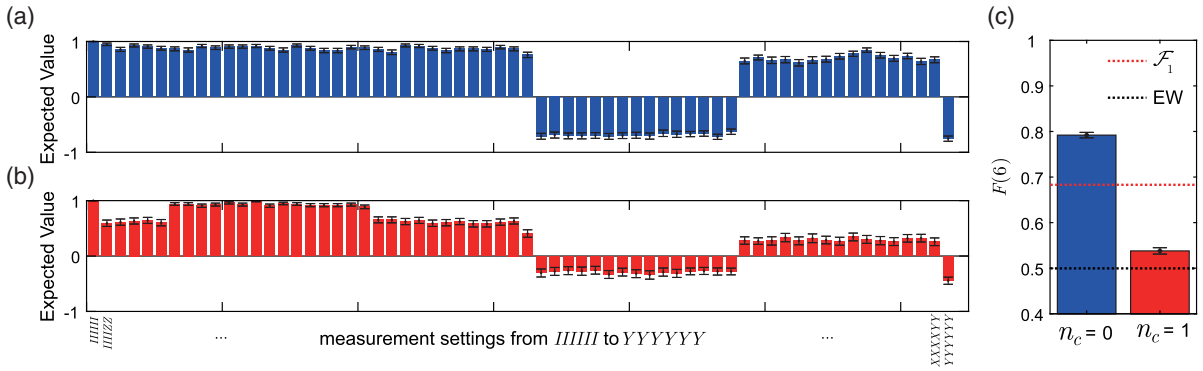

FIG. 2. Experimental results of network fidelity $F(6)$ of six-node network with classical node number $n_c = 0$ and $n_c = 1$ respectively. (a) The experimental results of network fidelity in the network with $n_c = 0$. (b) The experimental results of network fidelity measurement in the network with $n_c = 1$. (c) The calculated $F(6)$ from the results in (a) and (b). The black dashed line is the threshold of the EW, and the red dashed line is the threshold fidelity $\mathcal{F}_1$.

[Eq. (2)], the n_c untrusted nodes broadcast their results $\in \{+1, -1\}$ to achieve the maximal $F(N)$ [20]. The experimental results of $F(6)$ under the OCS are shown in Fig. 2(b), from which we calculate $F(6) = 0.538 \pm 0.007$ [shown with red bar in Fig. 2(c)]. As shown in Fig. 3(a), we can see that $F(6)$ either with $n_c = 0$ or $n_c = 1$ exceeds the EW threshold [44], which is strong evidence that the EW is no longer reliable in quantum network identification. However, with our criteria, the measured $F(6)$ does not exceed the threshold fidelity $\mathcal{F}_1$, which indicates there are classical nodes in the measured network. One may notice that, in the case of $n_c = 1$ under the OCS, $F(6) = 0.538 \pm 0.007$ is lower than $\mathcal{F}_3$ but higher than $\mathcal{F}_4$, where the fidelity threshold overcounts the number of classical nodes in the created network. This is caused by the imperfections in the state preparation, where $F(6) = 0.792 \pm 0.006$ in the case of $n_c = 0$, and such imperfections prevent us from achieving the optimal fidelity $\mathcal{F}_1 \simeq 0.6830$ with the OCS. These imperfections can be evaluated by our fidelity criteria in terms of the number of classical nodes. For $\mathcal{F}_4 < F(6) = 0.538 \pm 0.007 < \mathcal{F}_3$, the quantity of classical defects in the created network effectively equals to three classical nodes with the optimal mimicry.

We also experimentally prepare various N-node quantum networks with n_q up to 6 and n_c up to 18, where $N = n_q + n_c$ [20]. For each network, n_c nodes employ the OCS to achieve maximal network fidelity $F(N)$. The measured $F(N)$ are shown in Fig. 3(a). It is clear that $F(N)$ with n_c classical nodes are bounded by the threshold fidelity $\mathcal{F}_{n_c}$. One may notice that $F(N)$ decreases much faster than $\mathcal{F}_{n_c}$ as n_q is increased. This is mainly caused by

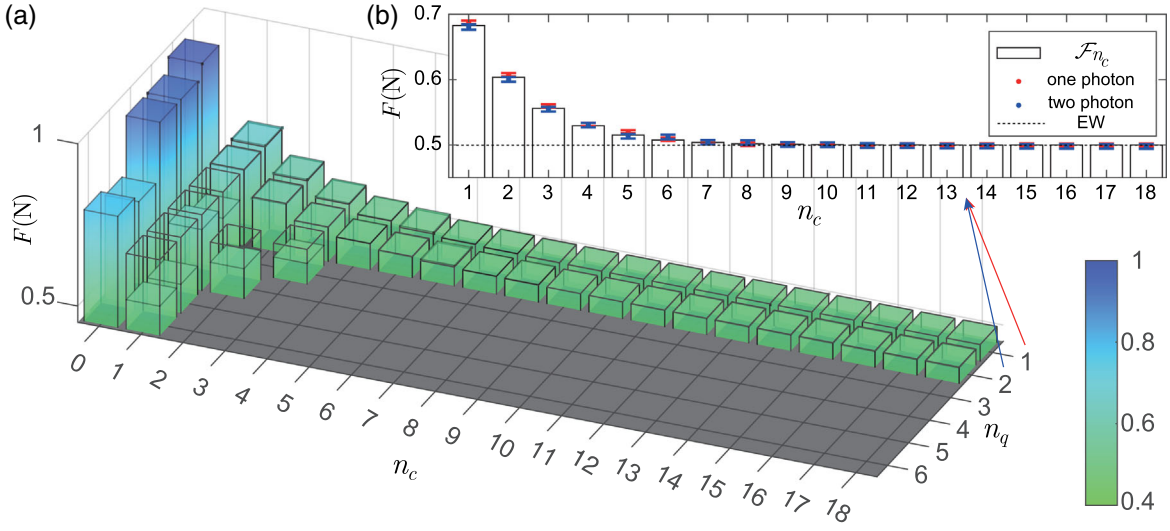

FIG. 3. Experimental results of network fidelity $F(N)$ in the network with variant quantum and classical node number n_q and n_c, respectively. (a) The bars edged with a black line represent the threshold of network fidelity $\mathcal{F}_{n_c}$. The filled color bars represent the experimental measured network fidelity $F(N)$ in its corresponding network. (b) The results of $F(N)$ in networks with $n_q = 1$ and $n_q = 2$. The bars represent $\mathcal{F}_{n_c}$, and red (blue) dots represent the measured $F(N)$ in the network with $n_q = 1$ ($n_q = 2$).

the imperfections in the state preparation, in which more imperfections are introduced when coherently manipulating more photons. When $n_q \geq 3$, $F(N)$ decreases below the EW threshold (0.5) quickly as n_c is increased ($n_c \geq 4$). We investigate $F(N)$ of networks with $n_q = 1$ and $n_q = 2$ for large n_c as the one-photon and two-photon states are prepared with high fidelities. The results of $F(N)$ for $n_q = 1$ and $n_q = 2$ are particularly shown in Fig. 3(b), from which we can see that $F(N)$ fits $\mathcal{F}_{n_c}$ very well. We analyze the standard deviation $\mathcal{E}$ of $F(N)$ in verifying entanglement and evaluating n_c. We observe $\mathcal{E} > 3$ when $n_c \leq 6$ in the created network with $n_q = 1$ and $n_q = 2$, which reflects a high confidence level of our criteria [20,31].

Our results, to the best of our knowledge, demonstrate the first method capable of counting the number of classical nodes in quantum networks. Moreover, the proposed method reveals that the quantum-classical hybrid networks with OCS can surpass the seminal EW threshold of $F > 1/2$, which causes serious flaws in using the verification of EW in quantum networks [44]. Our proof-of-principle photonic networking experiments, with n_q up to 6 and n_c up to 18, validated the proposed threshold network fidelities $\mathcal{F}_{n_c}$, and showed the failure of using an EW for genuine multipartite entanglement verification. Our results therefore not only open a new way to characterize classical defects in quantum networks [1–3,32–41] for a wide range of distributed quantum tasks [4–18], but also provide novel insights in multipartite nonclassical correlations in graph states [54–56]. We expect that our formalism could be extended to the other types of quantum states, such as W states, for the characterization of multipartite entanglement with further studies [42,43,57].

This work was supported by the National Natural Science Foundation of China (Grants No. 11975222, No. 61771443, No. U1738140, and No. 11974213), the National Key R&D Program of China (No. 2019YFA0308200), the Anhui Initiative in Quantum Information Technologies and the Chinese Academy of Sciences, the Shanghai Municipal Science and Technology Major Project (Grant No. 2019SHZDZX01) and Major Program of Shandong Province Natural Science Foundation (Grant No. ZR2018ZB0649). C.-M. L. is partially supported by the Ministry of Science and Technology, Taiwan, under Grant No. MOST 107-2628-M-006-001-MY4.

*yuaochen@ustc.edu.cn
†cmli@mail.ncku.edu.tw
‡pan@ustc.edu.cn
§These authors contributed equally to this work.

[1] S. Ritter, C. Nölleke, C. Hahn, A. Reiserer, A. Neuzner, M. Uphoff, M. Mücke, E. Figueroa, J. Bochmann, and G. Rempe, Nature (London) **484**, 195 (2012).
[2] H. J. Kimble, Nature (London) **453**, 1023 (2008).
[3] S. Wehner, D. Elkouss, and R. Hanson, Science **362**, eaam9288 (2018).
[4] M. Hillery, V. Bužek, and A. Berthiaume, Phys. Rev. A **59**, 1829 (1999).
[5] Y.-A. Chen, A.-N. Zhang, Z. Zhao, X.-Q. Zhou, C.-Y. Lu, C.-Z. Peng, T. Yang, and J.-W. Pan, Phys. Rev. Lett. **95**, 200502 (2005).
[6] D. Markham and B. C. Sanders, Phys. Rev. A **78**, 042309 (2008).
[7] B. A. Bell, D. Markham, D. A. Herrera-Martí, A. Marin, W. J. Wadsworth, J. G. Rarity, and M. S. Tame, Nat. Commun. **5**, 5480 (2014).
[8] H. Lu, Z. Zhang, L.-K. Chen, Z.-D. Li, C. Liu, L. Li, N.-L. Liu, X. Ma, Y.-A. Chen, and J.-W. Pan, Phys. Rev. Lett. **117**, 030501 (2016).
[9] C.-Y. Huang, N. Lambert, C.-M. Li, Y.-T. Lu, and F. Nori, Phys. Rev. A **99**, 012302 (2019).
[10] P. Kómár, E. M. Kessler, M. Bishof, L. Jiang, A. S. Sørensen, J. Ye, and M. D. Lukin, Nat. Phys. **10**, 582 (2014).
[11] T. J. Proctor, P. A. Knott, and J. A. Dunningham, Phys. Rev. Lett. **120**, 080501 (2018).
[12] R. Raussendorf and H. J. Briegel, Phys. Rev. Lett. **86**, 5188 (2001).
[13] P. Walther, K. J. Resch, T. Rudolph, E. Schenck, H. Weinfurter, V. Vedral, M. Aspelmeyer, and A. Zeilinger, Nature (London) **434**, 169 (2005).
[14] A. Broadbent, J. Fitzsimons, and E. Kashefi, in *Proceedings of the 2009 50th Annual IEEE Symposium on Foundations of Computer Science, FOCS '09* (IEEE Computer Society, Washington, DC, USA, 2009), pp. 517–526.
[15] S. Barz, E. Kashefi, A. Broadbent, J. F. Fitzsimons, A. Zeilinger, and P. Walther, Science **335**, 303 (2012).
[16] K. Chen and H.-K. Lo, Quantum Inf. Comput. **7**, 689 (2007).
[17] H.-K. Lo, M. Curty, and K. Tamaki, Nat. Photonics **8**, 595 (2014).
[18] M. Epping, H. Kampermann, C. Macchiavello, and D. Bruß, New J. Phys. **19**, 093012 (2017).
[19] M. Hein, J. Eisert, and H. J. Briegel, Phys. Rev. A **69**, 062311 (2004).
[20] See Supplemental Material at http://link.aps.org/supplemental/10.1103/PhysRevLett.124.180503 for the definition of graph states, the definition and discussions of classical nodes, the detailed derivation of the fidelity function, discussions on genuine multi-subsystem EPR steering, details of optimal cheating strategy (OSC) and its experimental setups and results, and details of statistical significance, which include Refs. [19,21–31].
[21] H. M. Wiseman, S. J. Jones, and A. C. Doherty, Phys. Rev. Lett. **98**, 140402 (2007).
[22] S. J. Jones, H. M. Wiseman, and A. C. Doherty, Phys. Rev. A **76**, 052116 (2007).
[23] C.-M. Li, K. Chen, Y.-N. Chen, Q. Zhang, Y.-A. Chen, and J.-W. Pan, Phys. Rev. Lett. **115**, 010402 (2015).
[24] M. A. Nielsen and I. L. Chuang, *Quantum Computation and Quantum Information* (Cambridge University Press, Cambridge, England, 2010).
[25] D. F. V. James, P. G. Kwiat, W. J. Munro, and A. G. White, Phys. Rev. A **64**, 052312 (2001).
[26] O. Gühne, G. Tóth, P. Hyllus, and H. J. Briegel, Phys. Rev. Lett. **95**, 120405 (2005).

[27] C.-M. Li, K. Chen, A. Reingruber, Y.-N. Chen, and J.-W. Pan, Phys. Rev. Lett. **105**, 210504 (2010).
[28] Q. Y. He and M. D. Reid, Phys. Rev. Lett. **111**, 250403 (2013).
[29] Y.-H. Kim, S. P. Kulik, M. V. Chekhova, W. P. Grice, and Y. Shih, Phys. Rev. A **67**, 010301(R) (2003).
[30] X.-C. Yao, T.-X. Wang, P. Xu, H. Lu, G.-S. Pan, X.-H. Bao, C.-Z. Peng, C.-Y. Lu, Y.-A. Chen, and J.-W. Pan, Nat. Photonics **6**, 225 (2012).
[31] B. Jungnitsch, S. Niekamp, M. Kleinmann, O. Gühne, H. Lu, W.-B. Gao, Y.-A. Chen, Z.-B. Chen, and J.-W. Pan, Phys. Rev. Lett. **104**, 210401 (2010).
[32] A. Pirker, J. Wallnöfer, and W. Dür, New J. Phys. **20**, 053054 (2018).
[33] T. E. Northup and R. Blatt, Nat. Photonics **8**, 356 (2014).
[34] C. Monroe, R. Raussendorf, A. Ruthven, K. R. Brown, P. Maunz, L.-M. Duan, and J. Kim, Phys. Rev. A **89**, 022317 (2014).
[35] A. Reiserer and G. Rempe, Rev. Mod. Phys. **87**, 1379 (2015).
[36] A. Sipahigil, R. E. Evans, D. D. Sukachev, M. J. Burek, J. Borregaard, M. K. Bhaskar, C. T. Nguyen, J. L. Pacheco, H. A. Atikian, C. Meuwly, R. M. Camacho, F. Jelezko, E. Bielejec, H. Park, M. Lončar, and M. D. Lukin, Science **354**, 847 (2016).
[37] N. Kalb, A. A. Reiserer, P. C. Humphreys, J. J. W. Bakermans, S. J. Kamerling, N. H. Nickerson, S. C. Benjamin, D. J. Twitchen, M. Markham, and R. Hanson, Science **356**, 928 (2017).
[38] P. C. Humphreys, N. Kalb, J. P. J. Morits, R. N. Schouten, R. F. L. Vermeulen, D. J. Twitchen, M. Markham, and R. Hanson, Nature (London) **558**, 268 (2018).
[39] K. S. Chou, J. Z. Blumoff, C. S. Wang, P. C. Reinhold, C. J. Axline, Y. Y. Gao, L. Frunzio, M. H. Devoret, L. Jiang, and R. J. Schoelkopf, Nature (London) **561**, 368 (2018).
[40] B. Jing, X.-J. Wang, Y. Yu, P.-F. Sun, Y. Jiang, S.-J. Yang, W.-H. Jiang, X.-Y. Luo, J. Zhang, X. Jiang, X.-H. Bao, and J.-W. Pan, Nat. Photonics **13**, 210 (2019).
[41] Y. Yu, F. Ma, X.-Y. Luo, B. Jing, P.-F. Sun, R.-Z. Fang, C.-W. Yang, H. Liu, M.-Y. Zheng, X.-P. Xie, W.-J. Zhang, L.-X. You, Z. Wang, T.-Y. Chen, Q. Zhang, X.-H. Bao, and J.-W. Pan, Nature (London) **578**, 240 (2020).
[42] R. Horodecki, P. Horodecki, M. Horodecki, and K. Horodecki, Rev. Mod. Phys. **81**, 865 (2009).
[43] O. Gühne and G. Tóth, Phys. Rep. **474**, 1 (2009).
[44] W. McCutcheon, A. Pappa, B. A. Bell, A. McMillan, A. Chailloux, T. Lawson, M. Mafu, D. Markham, E. Diamanti, I. Kerenidis, J. G. Rarity, and M. S. Tame, Nat. Commun. **7**, 13251 (2016).
[45] A. Pappa, A. Chailloux, S. Wehner, E. Diamanti, and I. Kerenidis, Phys. Rev. Lett. **108**, 260502 (2012).
[46] N. D. Mermin, Rev. Mod. Phys. **65**, 803 (1993).
[47] N. Brunner, D. Cavalcanti, S. Pironio, V. Scarani, and S. Wehner, Rev. Mod. Phys. **86**, 419 (2014).
[48] N. D. Mermin, Phys. Rev. Lett. **65**, 3373 (1990).
[49] A. Peres, Phys. Lett. **151A**, 107 (1990).
[50] A. Cabello, Phys. Rev. Lett. **101**, 210401 (2008).
[51] E. Amselem, M. Rådmark, M. Bourennane, and A. Cabello, Phys. Rev. Lett. **103**, 160405 (2009).
[52] G. Kirchmair, F. Zähringer, R. Gerritsma, M. Kleinmann, O. Gühne, A. Cabello, R. Blatt, and C. F. Roos, Nature (London) **460**, 494 (2009).
[53] A. J. Bennet, D. A. Evans, D. J. Saunders, C. Branciard, E. G. Cavalcanti, H. M. Wiseman, and G. J. Pryde, Phys. Rev. X **2**, 031003 (2012).
[54] T. Monz, P. Schindler, J. T. Barreiro, M. Chwalla, D. Nigg, W. A. Coish, M. Harlander, W. Hänsel, M. Hennrich, and R. Blatt, Phys. Rev. Lett. **106**, 130506 (2011).
[55] G. H. Aguilar, T. Kolb, D. Cavalcanti, L. Aolita, R. Chaves, S. P. Walborn, and P. H. Souto Ribeiro, Phys. Rev. Lett. **112**, 160501 (2014).
[56] L. Aolita, F. de Melo, and L. Davidovich, Rep. Prog. Phys. **78**, 042001 (2015).
[57] M. Walter, B. Doran, D. Gross, and M. Christandl, Science **340**, 1205 (2013).